Wavelength Tunable Distributed Bragg Reflector Laser Integrated with Electro-Absorption Modulator by a Combined Method of Selective Area Growth and Quantum Well Intermixing

ZHAO Ling-Juan*, ZHANG Jing, WANG Lu, CHENG Yuan-Bing, PAN Jiao-Qing, LIU Hong-Bo, ZHU Hon-Liang, ZHOU Fan, BIAN Jing, WANG Bao-Jun, ZHU Ning-Hua, Wei WANG

State Key Laboratory on Integrated Optoelectronics, Institute of Semiconductors, Chinese Academy of Sciences, P.O. Box 912, 100083 Beijing, PR China

Key Laboratory of Semiconductors Materials，Institute of Semiconductors, Chinese Academy of Sciences, P.O. Box 912, 100083 Beijing, PR China

ABSTRACT

Wavelength tunable electro-absorption modulated distributed Bragg reflector lasers (TEMLs) are promising light source in dense wavelength division multiplexing (DWDM) optical fiber communication system due to high modulation speed, small chirp, low drive voltage, compactness and fast wavelength tuning ability. Thus, increased the transmission capacity, the functionality and the flexibility are provided. Materials with bandgap difference as large as 250nm have been integrated on the same wafer by a combined technique of selective area growth (SAG) and quantum well intermixing (QWI), which supplies a flexible and controllable platform for the need of photonic integrated circuits (PIC). A TEML has been fabricated by this technique for the first time. The component has superior characteristics as following: threshold current of 37mA, output power of 3.5mW at 100mA injection and 0V modulator bias voltage, extinction ratio of more than 20 dB with modulator reverse voltage from 0V to 2V when coupled into a single mode fiber, and wavelength tuning range of 4.4nm covering 6 100-GHz WDM channels. A clearly open eye diagram is observed when the integrated EAM is driven with a 10-Gb/s electrical NRZ signal. A good transmission characteristic is exhibited with power penalties less than 2.2 dB at a bit error ratio (BER) of 10^{-10} after 44.4 km standard fiber transmission.

Key words: Tunable lasers, Distributed Bragg reflector lasers, Electroabsorption modulator, Quantum-well intermixing, Selective area growth

1. INTRODUCTION

Wavelength tunable electro-absorption modulated DBR lasers (TEML) are very attractive components in long haul

* Email: Ljzhao@semi.ac.cn, 86-10-82304437 (O)

Semiconductor Lasers and Applications III,
edited by Lianghui Chen, Hiroyuki Suzuki, Paul T. Rudy, Ninghua Zhu,
Proc. of SPIE Vol. 6824, 68240N, (2007) · 0277-786X/07/$18 · doi: 10.1117/12.784832

WDM fiber optic communication system as they are compact, potentially low-cost, and can facilitate low-drive voltages with high-modulation bandwidth [1]. Compared with bulk electro-absorption modulators employing Franz–Kelydsh effect, quantum-well electro-absorption modulators (QW-EAMs) using the quantum confined Stark effect (QCSE) can offer increased efficiency [2]. Additionally, QW-EAMs can enable negative-chirp operation for efficient transmission at high bit-rates, where fiber dispersion is increasingly important.

The key issue for the fabrication of monolithic photonic integrated circuits is the combination of different functional sections (active or passive) on a single epitaxial wafer, which requires the definition of regions with different bandgap wavelengths. In the case of TEML, three different bandgap wavelengths are needed: one for the gain region, one for the modulator region and one for the grating and phase region, with relation of $\lambda_{gain}>\lambda_{modulator}>\lambda_{grating}$. To integrate different materials on the same wafer, the most popular methods are selective area growth (SAG) [3], quantum well intermixing (QWI) [4], butt-joint [5], and single-mode vertical integration (SMVI) [6]. Although the butt-joint regrowth process does facilitate high flexibility, it requires overcritical etching and re-growth steps .The difficulty associated with matching the thickness and achieving the desired composition to avoid reflection and loss at the interface is great [7].And SMVI needs special waveguide design, longer chip size and rigorous etching process. Both of them require complex fabrication techniques and are hard to realize efficient optical coupling between different sections.

SAG allows simultaneous epitaxy on a patterned substrate with different growth rate and results in the growth of quantum wells with different thickness, therefore the definition of sections with different bandgap wavelengths. By locally introducing different SiO2 pattern, much more than three bandgap wavelengths can be realized in the same SAG growth, which is sufficient for the fabrication of TEML. However, the main drawback of SAG is that there exists transition area between different sections with typical length of several tens of microns limited by the surface diffusion of the growth constituents. The transition area has gradually changed bandgap wavelengths, thus the optical absorption loss in the transition area may be high. In addition, the optical mode overlap with the MQW may be not ideal in all sections due to the thickness variation.

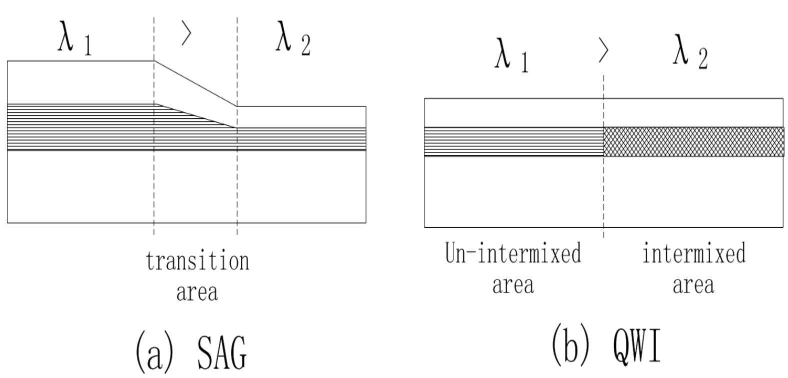

Fig1 Schematic view of selective area growth and quantum-well intermixing

QWI which is relatively simple relies on selective partial material inter-diffusion between the well and barrier induced by impurities or vacancies during a post-growth anneal process, and results in a change of QW shape and transition energies. QWI has high space resolution (several microns) and abrupt bandgap wavelength change between different sections. A schematic view of selective area growth and quantum-well intermixing process is show in Fig.1. Although an all-SAG method can be used to fabricate TEML, we adopt a combined process of SAG and QWI in this work. There are two benefits of our method compared with the former one: 1) we can adopt the same quantum well structure and growth condition which we used to fabricate integrated DFB laser and EA modulator before [8], thus ease the fabrication process; 2) QWI process results in an abrupt bandgap wavelength change between different sections, thus reduces absorption loss in the transition area. The QWI process has been well established in our group [9].

2. DEVICE FABRICATION

A schematic illustration of the tunable EA-DBR chip is shown in Fig.2. The device consists of five separate sections: a 250 μm rear mirror, a 300 μm gain section, a 100 μm phase section, a 50 μm front mirror and a 150 μm EA modulator. Trenched isolation regions separating each sections are all the same 50 μm long.

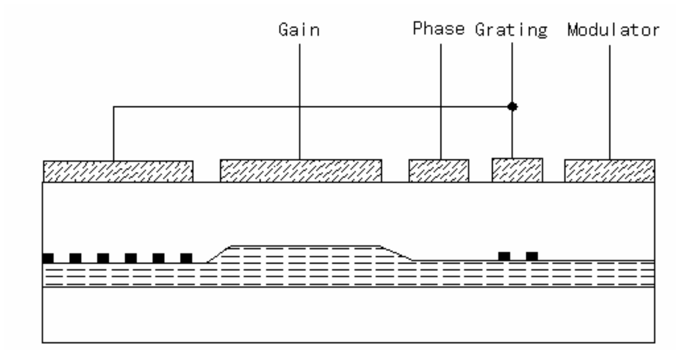

Fig.2 Schematic cross section of the EA-modulated tunable DBR laser

First, a SiO_2 dielectric film with typical thickness of 150nm by PECVD was deposited on (100)-oriented n-InP substrate. Then, stripe patterns were defined in the SiO_2 mask by conventional photolithography and chemical etching at gain sections. The strips were formed along the [110] direction. Both the mask strip width and the open stripe width are 15 μm . An n-InP buffer layer, MQW active waveguide layers and an i-InP implant buffer layer were then grown in turn by low pressure MOCVD on this patterned substrate. The InGaAsP MQWs consisted of 7 periods 6 nm compressively strained (0.4%) wells, separated by 9 nm tensile-strained (-0.2%) barriers, which was sandwiched between 100 nm lower and upper separated confinement cladding layers. The as-grown MQWs had a PL peak wavelength of 1.560 μm at gain region and that of 1.502 μm at other regions. Then P^+ ions were implanted into the surface of whole wafer except gain and modulator regains with ion energy of 50 KeV and dose of 5×10^{13} cm^{-3}. After re-depositing a fresh SiO_2 layer on the whole wafer, a thermal anneal of 2 minutes at temperatures of 700 °C was performed to induce QWI process. As a result of QWI, a near 100 nm wavelength blue-shift occurred at P^+ Ions implanted sections. A detail wavelength change of different sections after the whole process is shown in Fig.3.

By a combined method of SAG and QWI, we had accomplished three different wavelengths to meet the need of different functional sections on the same single epi-wafer (1560 nm for gain section of LD, 1502 nm for modulator and 1406 nm for grating/phase), and there was no distinct change of intensity and FWHM of PL at non P^+ implanted sections after thermal anneal, which means that QWI process does not deteriorate the MQW quality of the regions which are not to be intermixed. The grating, which was localized at the mirror sections, was realized by convenient holographic lithography followed by dry and wet etching. The reflectivity of the rear- and front- grating are over 80% and 10% respectively. The grating coupling coefficient κ is about 70 cm^{-1}. Finally, p-InP layer and p^+-InGaAs contact layer was grown over the whole wafer.

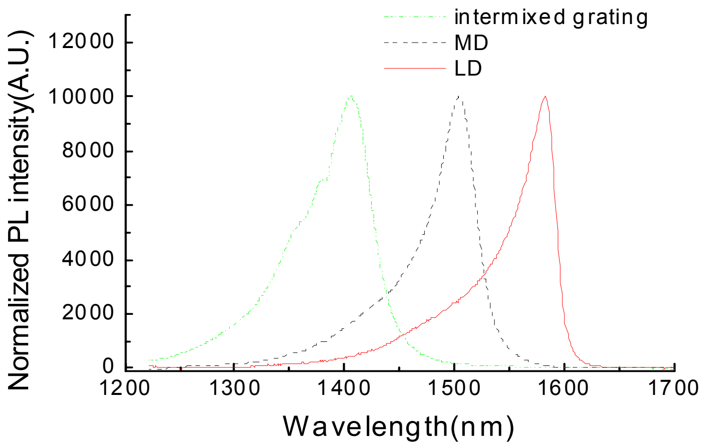

Fig.3 PL spectrum of different region after thermal anneal at 700°C for 2 minutes

A standard 2-μm-wide single-mode ridge waveguide was etched to 100 nm above the waveguide core. Electrical isolation between the different sections was accomplished by a selective wet etching off the InGaAs contact layer and performing a deep He^+ implantation. To reduce the junction capacitance of modulator, a 8 μm deep-ridge was etched down over MQW active layers. Passivation and electrical isolation of ridge sidewalls was accomplished through a 400-nm-thick SiO_2 layer. A standard Ti-Pt-Au metal was sputtered and p-electrode pattern was formed by lift-off approach. For further decreasing parasitic capacitance of modulator, a 3-μm-thick polyimide layer was performed under the modulator bonding pad to serve as a low–K dielectric. Then, the wafer was thinned and Au-Ge-Ni contact was performed on the n-side. Finally, after cleaving to bars, AR coating was formed on the modulator output facet.

3. DEVICE PERFORMANCE

The light output power versus gain section current (P-I) performance at various bias voltage of modulator is shown in Fig.4, which is tested under room temperature using an integral sphere. The TEML has a threshold current I_{th} of 37 mA. The 50-μm-long isolation trench between different laser sections should be further shorten to reduce internal optical loss in laser cavity, and thus reduce I_{th}. There was no observable change in I_{th} and the wavelength of the output light over the entire range of the modulator bias voltage, which indicates sufficient electrical isolation of the laser and modulator sections. With modulator in open circuit state, the CW output power is 3.5 mW at I_{gain}=100 mA, $I_{grating}$=0 and I_{phase}=0.

The output power is coupled into single mode fiber with coupling efficiency of 15%, and DC extinction characteristic is presented in Fig.4 in the condition of I_{gain}=100mA, $I_{grating}$=0 and I_{phase}=0. More than 20 dB extinction ratio was demonstrated with modulator reverse bias increasing from 0v to 2 . We find a great increase in the extinction ratio comparing with measuring by integral sphere, which is due to some un-modulated scattering light is collected by integral sphere and deteriorate the measured extinction ratio.

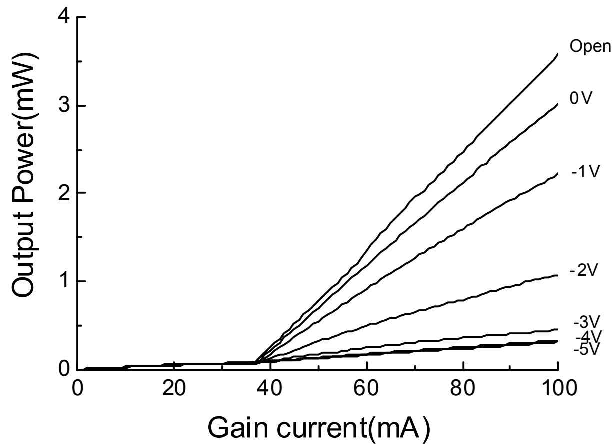

Fig.4 P-I characteristics of the TEML at different modulator bias voltage measured by integral sphere

Fig.5 shows the tuning performance of the TEML. The optical spectrum has 4.4 nm tuning range, which covers 6 channels on 100 GHz WDM grid: the channel wavelengths are 1554.94 nm, 1554.13 nm, 1553.33 nm, 1552.52 nm, 1551.72 nm, 1550.92 nm. DC side-mode suppression ratio (SMSR) keeps greater than 35 dB over the total tuning range. We observe no significant variation of extinction ratio when the laser wavelength is tuned to a given channel, which is due to the small wavelength tuning range

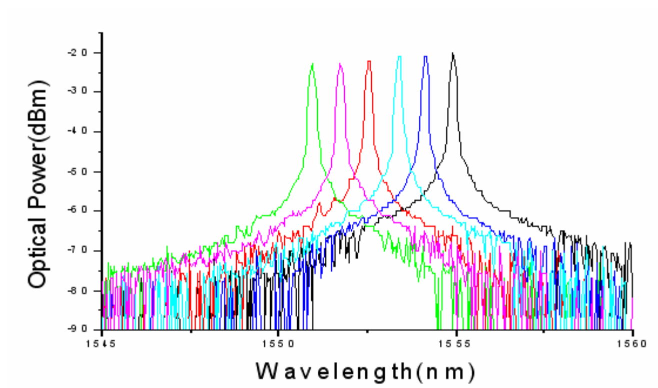

Fig.5 The tuning spectra for TEML showing 6 channels spaced at 100GHz WDM grid over a 4.4nm tuning range. The SMSR is greater than 35dB over the entire tuning range

The small signal electrical to optical frequency response of the modulator with the DBR laser operated CW is measured and is shown in Fig.6. The reverse bias voltage of modulator is 3 V and the laser current is 120 mA. The frequency response rolls off smoothly with a 3-dB frequency bandwidth of 8 GHz.

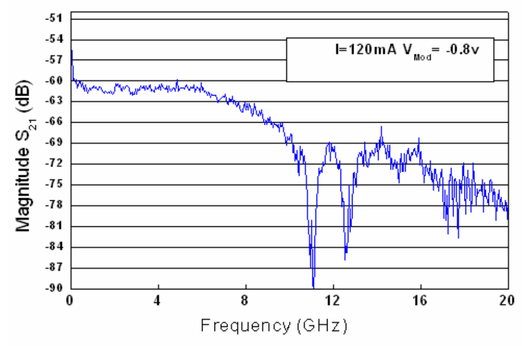

Fig.6 Small signal response of the integrated device.

To demonstrate the high-speed performance of the integrated device, 10-Gb/s non-return to zero (NRZ) with a pseudorandom bit sequence (PRBS) of 2^{31}-1 transmission experiment is taken in standard single-mode fiber. Fig.7 presents eye diagrams of the back to back and 44.4 km transmission at 10-Gb/s NRZ electrical signal. The eye diagrams are open and clear with dynamic extinction ratios (ER) over 8.8 dB.

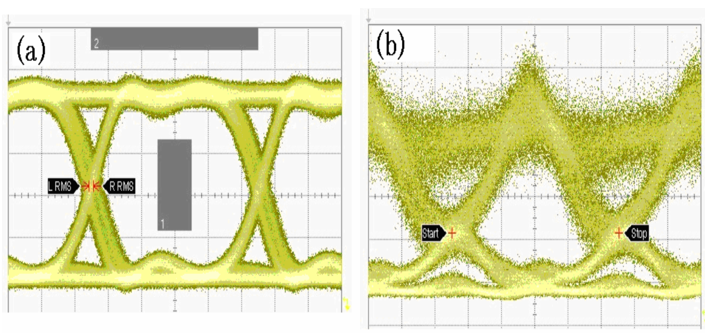

Fig.7 10-Gb/s NRZ pattern (a) back to back (b) transmission 44.4km eye diagram of the integrated device.

The BER performance is summarized in Fig.8. The receiver sensitivity, measured at a bit error ratio (BER) of 10^{-10}, is from -20.1 for back to back to -17.9 dBm for 44.4 km transmission. Power penalty of less than 2.2 dB is obtained for BER of 10^{-10} after 44.4 km standard fiber transmission.

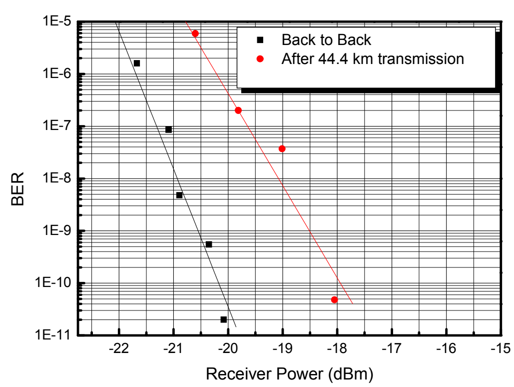

Fig.8 BER performance of the integrated device at 10-Gb/s.

4. CONCLUSION

A combined method of SAG and QWI was successfully utilized to realize tunable electro-absorption modulated DBR laser for the first time. Without extra epitaxial regrowth, three functional sections with different wavelengths are integrated on the same wafer. The integrated devices achieve superior characteristics as following: threshold current of 37 mA, output power of 3.5 mW at 100mA laser driving current and 0V modulator bias voltage, extinction ratio of more than 20 dB with modulator reverse voltage from 0V to 2V when coupled into a single mode fiber, and wavelength tuning range of 4.4 nm covering 6 channels on a 100-GHz grid for WDM telecommunications. A clearly open eye diagram is obtained with over 8 dB dynamic extinction ratio. Power penalty less than2.2 dB has been obtained after transmission through 44.4 km of the standard fiber. It verifies that this approach simplifies fabrication process without significantly compromising the performance of the device, and therefore is a promising technique in the fabrication of photonic integrated circuits.

REFERENCES

1. M. Okayasu *et al.*, "A 1550-nm 40-Gb/s electro-absorption DFB laser diode module for transponders with very short reach (< 2 km) applications," *LEOS Tech. Dig.*, 513–514 (2004).
2. M. K. Chin, "Comparative analysis of the performance limits of Franz–Keldysh effect and quantum confined Stark effect electroabsorption waveguide modulators," *Proc. Inst. Electr. Eng.—Optoelectro*n. 142(2), 109–114 (1995).
3. Morvan M., Sorel Y., Delprat D. and Ramdane, "A. 10 Gbit/s transmission over 75 km standard fiber using a tunable laser-modulator based on the identical active layer approach," *ECOC Conference Publication*, No. 448 (1997).
4. Mason B., Fish G. A., DenBaars S. P. and Coldren L. A, "Widely tunable Sampled Grating DBR laser with integrated electroabsorption modulator." *IEEE Photon. Technol. Lett*. 1(6), 638 (1999).
5. Johnson J. E., Ketelsen L. J.-P., Ackerman D. A. *et al.*, "Fully stabilized electroabsorption-modulated tunable DBR laser transmitter for long-haul optical communications," *IEEE J. Sel. Top. Quantum Electron.* 7(2), 168 (2001).
6. Raring J. W., Skogen E. J., Johansson L. A. *et al,* "Demonstration of widely tunable single-chip 10-Gb/s laser-modulators using multiple-bandgap InGaAsP quantum-well intermixing," *IEEE Photon. Technol. Lett*. 16(7), 1613 (2004).
7. Zhang J., Lu Y., and Zhao L. J. *et al,* "An integratable distributed bragg reflector laser by low-energy ion implantation induced quantum well intermixing," *Chin J. Semiconductor*. 25, 889 (2004).
8. Li B. X., Hu X. H., Zhu H. L. and Wang W. *et al,* "Integrated electroabsorption-modulated DFB lasers by using an improved butt-joint method," *Chin Opti Lett*. 2(4), 226 (2004).
9. Li B. X., Hu X. H., Zhu H. L. and Wang W. *et al,* "Monolithically Integrated DFB-LD/EA-MD light Source for 10Gbit/s Transmission," Chin J. Semiconductor (accepted).